



# Age-related increases in PGD<sub>2</sub> expression impair respiratory DC migration, resulting in diminished T cell responses upon respiratory virus infection in mice

Jincun Zhao,<sup>1</sup> Jingxian Zhao,<sup>1,2</sup> Kevin Legge,<sup>3</sup> and Stanley Perlman<sup>1</sup>

<sup>1</sup>Department of Microbiology, University of Iowa, Iowa City, Iowa, USA. <sup>2</sup>Institute for Tissue Transplantation and Immunology, Jinan University, Guangzhou, China. <sup>3</sup>Department of Pathology, University of Iowa, Iowa City, Iowa, USA.

**The morbidity and mortality associated with respiratory virus infection is felt most keenly among the elderly. T cells are necessary for viral clearance, and many age-dependent intrinsic T cell defects have been documented. However, the development of robust T cell responses in the lung also requires respiratory DCs (rDCs), which must process antigen and migrate to draining LNs (DLNs), and little is known about age-related defects in these T cell-extrinsic functions. Here, we show that increases in prostaglandin D<sub>2</sub> (PGD<sub>2</sub>) expression in mouse lungs upon aging correlate with a progressive impairment in rDC migration to DLNs. Decreased rDC migration resulted in diminished T cell responses and more severe clinical disease in older mice infected with respiratory viruses. Diminished rDC migration associated with virus-specific defects in T cell responses and was not a result of cell-intrinsic defect, rather it reflected the observed age-dependent increases in PGD<sub>2</sub> expression. Blocking PGD<sub>2</sub> function with small-molecule antagonists enhanced rDC migration, T cell responses, and survival. This effect correlated with upregulation on rDCs of CCR7, a chemokine receptor involved in DC chemotaxis. Our results suggest that inhibiting PGD<sub>2</sub> function may be a useful approach to enhance T cell responses against respiratory viruses in older humans.**

## Introduction

Many age-dependent defects in the immune response to pathogens have been identified and shown to correlate with worse outcomes after infection with such pathogens as influenza A virus (IAV), West Nile virus, and, most notably, severe acute respiratory syndrome coronavirus (SARS-CoV) (1–4). More than 90% of all deaths from IAV occur in the elderly (>65 years of age) (5). In the 2002–2003 SARS epidemic, no patients under 24 years of age died, while mortality was more than 50% in those over 65 years of age (6). Since T cells are necessary for virus clearance in infected animals, prior studies have focused on virus-specific T cell responses in order to understand this age-dependent increase in susceptibility. Oligoclonal expansions of virus-specific T cells, holes in the T cell repertoire, and quantitative and qualitative defects in T cell function in aged hosts have been demonstrated previously (1, 2, 7).

The development of a robust antiviral T cell response in the lungs requires efficient pathogen recognition and activation and migration of respiratory DCs (rDCs) to the draining LNs (DLNs), in which the T cell response is primed. Defects in DC function have been identified in some, but not all, studies of older populations. Most of these studies analyzed Langerhans cells (skin and mucosal DCs) *in vivo* in mice or were performed *in vitro* using human or mouse DCs (8–10). Little is known about age-dependent changes in the lung environment that might impact rDC migration or function and consequently diminish the T cell priming ability of these cells (7). Candidate molecules that might vary in

expression and affect rDC migration include chemokines, such as CCL19 and CCL21 (11), and eicosanoids, pleiotropic bioactive lipid mediators (12, 13). The latter include prostaglandins and leukotrienes, which have been implicated in DC migration from sites such as the skin to the DLNs. For example, the cysteinyl leukotriene LTC<sub>4</sub> is involved in DC migration from the skin to DLNs but is not required for rDC migration to the lung DLNs (14, 15). Whether lipid mediators are involved in migration from the lungs to the DLNs in young or aged animals infected with viruses or other pathogens is unknown.

To determine the relative importance of deficiencies in T cell- or rDC-intrinsic function compared with that of the lung environment in older mice, we infected animals with several respiratory viral pathogens, including IAV, SARS-CoV, respiratory syncytial virus (RSV), and a pneumotropic strain of mouse hepatitis virus (MHV-1). Like IAV and SARS-CoV, RSV causes severe disease in elderly patients (16). MHV-1 causes a severe acute respiratory disease in mice (17). We show, for the first time to our knowledge, that the ability of rDCs to migrate to DLNs is compromised in aged mice, with a decline in migration occurring as early as 6 months of age. Diminished rDC migration correlated with defects in virus-specific T cell responses and was not cell intrinsic but rather reflected age-dependent changes in the lung environment. Specifically, we show that defects in rDC migratory ability correlated with an age-dependent increase in levels of prostaglandin D<sub>2</sub> (PGD<sub>2</sub>). Treatment with PGD<sub>2</sub> antagonists reversed this defect in rDC migration, with concomitant enhancement of the antiviral T cell response and prolonged survival. This effect correlated with upregulated expression of CCR7, a chemokine receptor involved in DC chemotaxis.

**Conflict of interest:** The authors have declared that no conflict of interest exists.

**Citation for this article:** *J Clin Invest.* 2011;121(12):4921–4930. doi:10.1172/JCI59777.

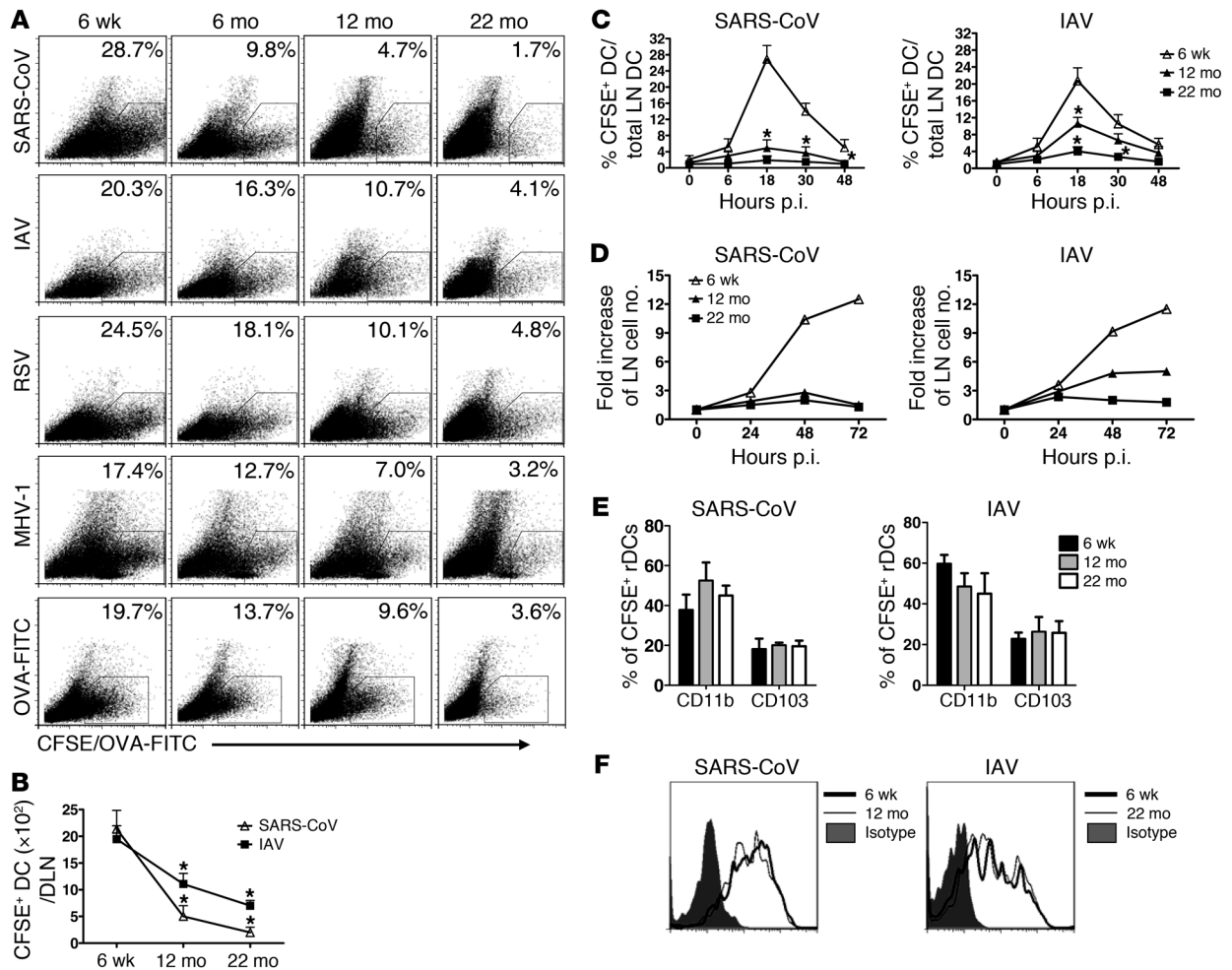


**Figure 1** rDC migration to DLNs progressively decreases in aged mice. (A) Six-week-old, six-month-old, twelve-month-old, and twenty-two-month-old mice were i.n. inoculated with 50  $\mu$ l 8 mM CFSE. Six hours after instillation, mice were infected with SARS-CoV, IAV, RSV, or MHV-1. Naive mice inoculated with 200  $\mu$ g/75  $\mu$ l OVA-FITC served as controls. After 18 hours, single-cell suspensions were prepared from lung DLNs. The numbers represent the percentage of CFSE<sup>+</sup> cells within the CD11c<sup>+</sup>MHCII<sup>+</sup> DC population per LN. (B) Total CFSE<sup>+</sup> DC numbers per LN, (C) the time course of rDC migration to the DLNs, (D) fold increase in DLN cellularity relative to that of naive mice, and (E) the proportion of CD11b<sup>+</sup> and CD103<sup>+</sup> populations among CFSE<sup>+</sup>CD11c<sup>+</sup>MHCII<sup>+</sup> rDCs in DLNs are also shown. (F) CD86 expression on rDCs in the lung 18 hours p.i. *n* = 4 mice in each group for each experiment. Data are representative of 5–10 independent experiments. \**P* < 0.05 versus 6 week.

**Results**

*rDC migration to DLNs progressively decreases as mice age.* We analyzed rDC migration to DLNs in the context of respiratory infections caused by SARS-CoV (mouse-adapted MA15 strain), IAV (PR8 strain), RSV (A2 strain), and MHV-1. C57BL/6 (B6) mice were inoculated i.n. with CFSE to label rDCs and infected 6 hours later. Frequency and numbers of CFSE<sup>+</sup> rDCs in the DLNs were determined at 18 hours postinfection (p.i.) (gating shown in ref. 18), the time of peak rDC migration in most (18–21) but not all studies (22). In all 4 infections, there was a progressive decrease in frequencies and numbers of rDCs in the DLNs as mice aged (Figure 1, A and B). We also measured rDC migration at other times p.i. and confirmed that the peak of rDC migration remained at 18 hours p.i. at all ages (Figure 1C). Enhanced rDC migration resulted in increased cellularity in the DLNs of 6-week-old mice, with only modest change or no changes in cell numbers detected in the

DLNs of 12-month-old and 22-month-old infected mice (Figure 1D). Decreased rDC migration did not occur only in the context of infection, because fewer rDCs were detected in the DLNs of uninfected aged mice after labeling with OVA-FITC, a intervention that also induces rDC activation and migration (ref. 23 and Figure 1A). Notably, age-dependent decreases in rDC migration were most striking in mice infected with SARS-CoV, with profound defects observed even in 6-month-old mice. For subsequent experiments, we analyzed mice infected with SARS-CoV or IAV.

CD11b<sup>+</sup> and CD103<sup>+</sup> rDCs are the most important rDCs for T cell priming in the DLN (24–27) and differences in migration of each subset could contribute to differences in T cell responses. However, this was not the case, because similar proportions of the 2 rDC subsets were detected in the DLNs of 6-month-old, 12-month-old, and 22-month-old SARS-CoV- and IAV-infected mice (Figure 1E). To assess differences in rDC activation during

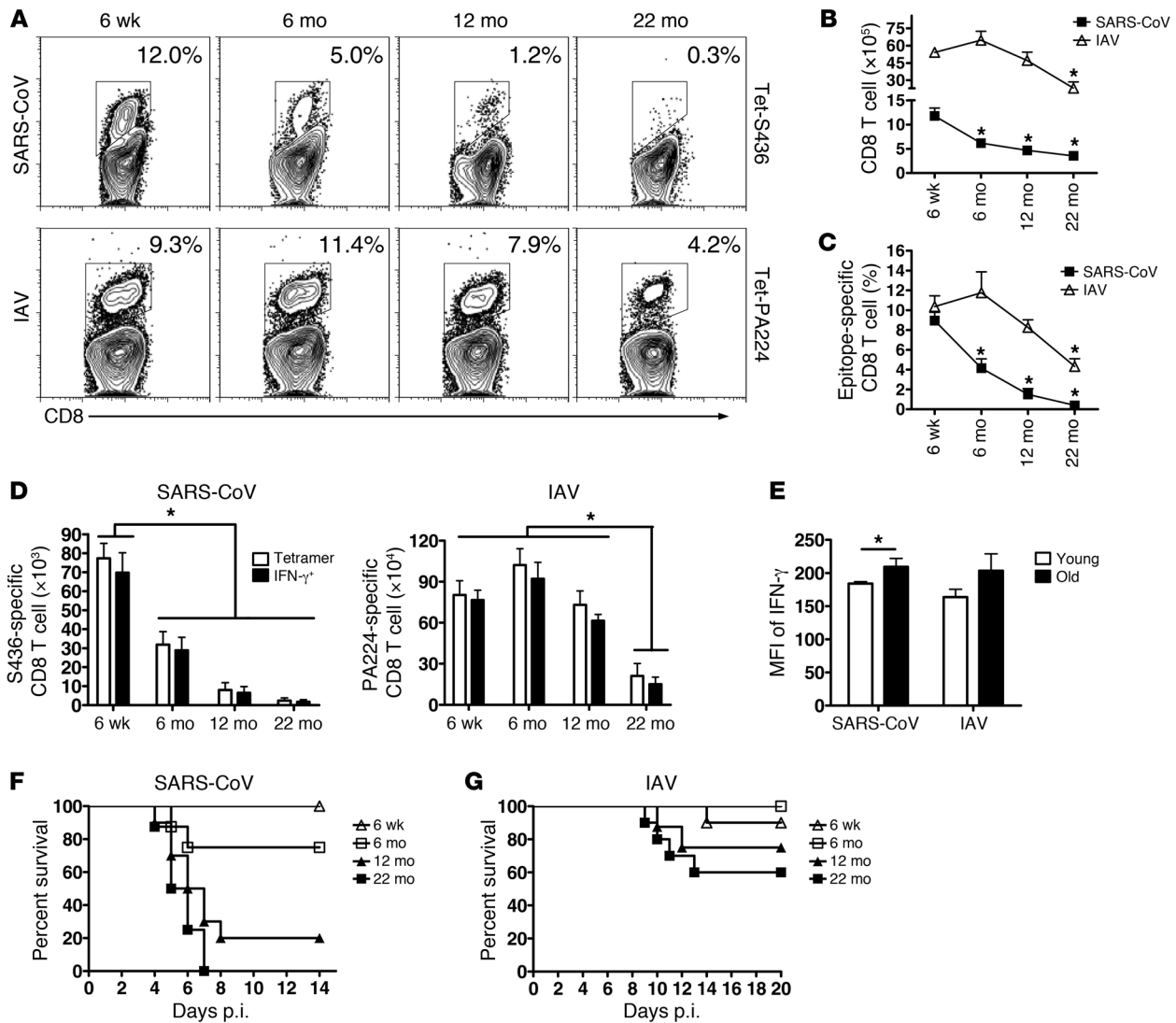


**Figure 2**

Age-dependent decreases in virus-specific CD8 T cell responses in lungs of SARS-CoV- and IAV-infected mice. Lung cells were harvested from young and aged B6 mice 6 days or 8 days after SARS-CoV or IAV infection, respectively. (A) Tetramer staining for epitopes S436 (Tet-S436) and PA224 (Tet-PA224) (numbers represent the percentage of tetramer<sup>+</sup> CD8 T cells), (B) total numbers of CD8 T cells, and (C) frequency and (D) numbers of tetramer<sup>+</sup> or IFN-γ<sup>+</sup> virus-specific CD8 T cells for epitopes S436 and PA224 are shown. \**P* < 0.05. (E) Geometric mean of fluorescence intensity (MFI) of IFN-γ production upon peptide stimulation is shown (young, 6 weeks old, SARS-CoV infected and 22 months old, IAV infected). *n* = 4–6 mice/group/experiment; \**P* < 0.05. Data are representative of 4–5 independent experiments. Mice of various ages were i.n. infected with (F) SARS-CoV or (G) IAV virus. Mortality was monitored daily. *P* values were determined by Kaplan-Meier survival tests (for SARS-CoV-infected mice, 6-week-old mice, *n* = 14; 6-month-old mice, *n* = 8; 12-month-old mice, *n* = 10; 22-month-old mice, *n* = 8; for 6-week-old versus 12-month-old or 22-month-old, *P* < 0.005) (for IAV-infected mice, 6-week-old mice, *n* = 10; 6-month-old mice, *n* = 8; 12-month-old mice, *n* = 8; 22-month-old mice, *n* = 10; for 6-week-old versus 22-month-old mice, *P* = 0.04).

aging, we measured CD86 (Figure 1F) and CD40 (data not shown) expression on rDCs harvested from lungs. rDC activation was equivalent in 6-week-old, 12-month-old, and 22-month-old mice, again suggesting that the predominant defect in these cells was inability to migrate to the DLNs. rDCs must uptake, process, and present antigen to prime T cells. The possible role of age-dependent defects in antigen uptake and processing was examined by treating uninfected mice with OVA-DQ, an antigen that becomes fluorescent only after proteolysis in the cell. Antigen uptake and processing were equivalent in young and aged mice, as evidenced

by similar frequencies of OVA-FITC<sup>+</sup> or OVA-DQ<sup>+</sup> CD11b and CD103 rDCs in the infected lung (Supplemental Figure 1A; supplemental material available online with this article; doi:10.1172/JCI59777DS1). There was an age-dependent decrease in the fraction of OVA-DQ<sup>+</sup> rDCs in the DLNs of 22-month-old mice (Supplemental Figure 1B). However, consistent with a rDC migration defect, no notable differences were observed when mice treated with OVA-FITC or OVA-DQ were compared (Supplemental Figure 1B), suggesting equivalent ability to process antigen. Further, OVA-FITC-loaded rDCs from 6-week-old and 22-month-old mice

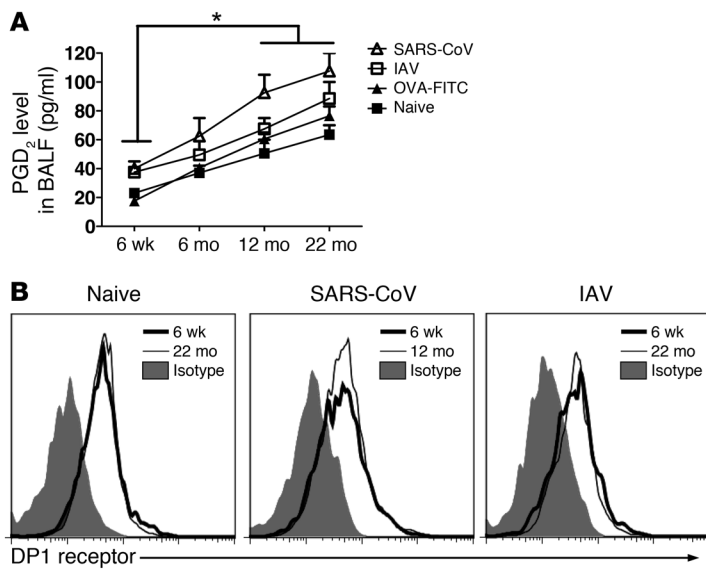


**Figure 3**

Elevated levels of PGD<sub>2</sub> in uninfected and infected aged mice. (A) An enzyme immunoassay was used to quantify PGD<sub>2</sub> levels in the BALF, following the manufacturer's instructions. *n* = 4 mice in each age per experiment. Data are representative of 3 independent experiments. \**P* < 0.05. (B) DP1 receptor expression on rDCs harvested from the lungs of naive mice or mice at 18 hours after infection with SARS-CoV or IAV was measured, as described in Methods. Data are representative of 3 independent experiments.

showed similar ability to stimulate proliferation of naive OT-1 cells in a 4-day in vitro proliferation assay (Supplemental Figure 1C).

*Age-dependent decreases in virus-specific CD8 T cell responses in lungs of SARS-CoV- and IAV-infected mice.* Defects in rDC migration to the DLN are predicted to result in diminished T cell responses. To assess this possibility, we examined virus-specific CD8 T cell responses in the lungs of 6-week-old, 6-month-old, 12-month-old, and 22-month-old mice infected with SARS-CoV or IAV using MHC class I/peptide tetramers. rDC migration was decreased in SARS-CoV-infected 6-month-old mice (Figure 1A), and, concomitantly, total and epitope S436-specific CD8 T cell responses were also decreased compared with those of 6-week-old mice (Figure 2, A–D). SARS-CoV-specific T cell responses continued to decrease as mice aged, so that responses were reduced by approximately 90% at 12 months of age compared with those of infected mice at 6 weeks of age. By 22 months of age, virtually no virus-specific CD8 T cells were identified in SARS-CoV-infected lungs.

In IAV-infected mice, we observed decreases in the frequency and number of PA224-specific CD8 T cells in the lungs, with the most dramatic effects in 22-month-old mice (Figure 2, A–D). For these experiments, we primarily analyzed the PA224-specific CD8 T cell response. There was also a very dramatic decrease in the numbers of CD8 T cells responding to the NP366 epitope as mice aged (Jincun Zhao, unpublished observations), but this decrease may reflect, in large part, an age-dependent hole in the T cell repertoire (1). Tetramer S436<sup>+</sup> and PA224<sup>+</sup> CD8 T cells were functional in old mice, since they expressed IFN- $\gamma$  after peptide stimulation at the same or higher levels as CD8 T cells isolated from 6-week-old mice (Figure 2, D and E).

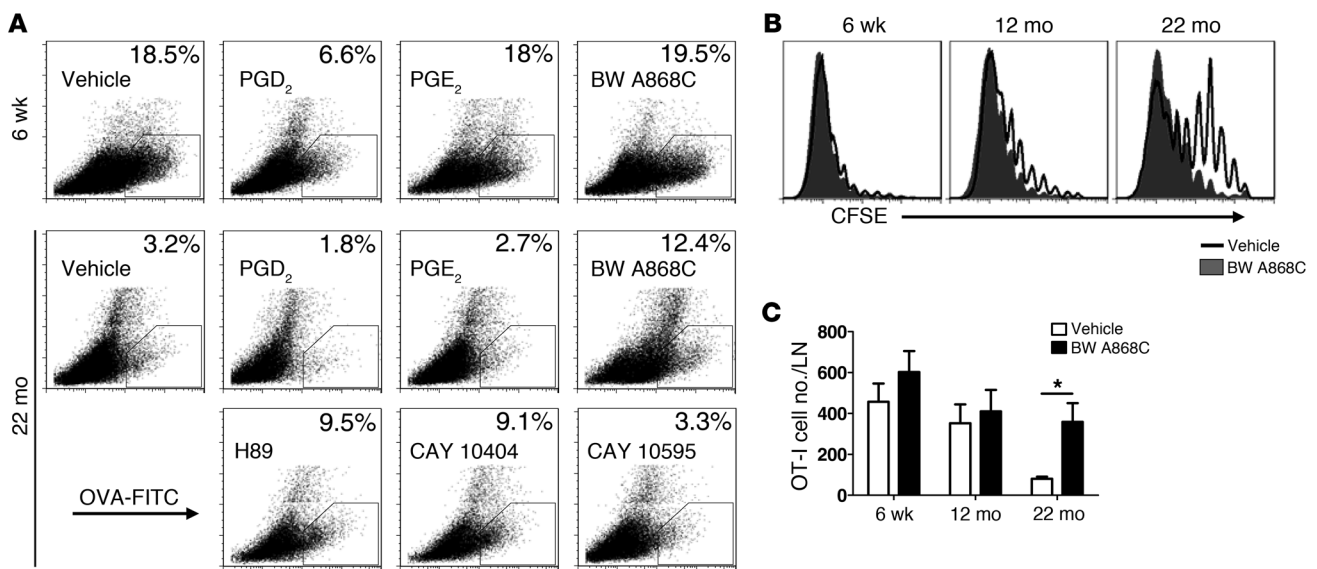
To investigate further whether any T cell-intrinsic loss of function occurred in 12-month-old mice, we performed a set of adoptive transfer experiments, in which naive splenocytes from 6-week-old and 12-month-old mice were transferred to 6-week-old and 12-month-old Thy1-mismatched mice prior to SARS-CoV infection. T cell frequency and function in the lungs was assessed by intracellular IFN- $\gamma$  production. As shown in Supplemental Figure 2A, epitope S436-specific CD8 T cells from 6-week-old and 12-month-old mice were present at similar frequencies in the lungs of 6-week-old mice. In contrast, we

detected greatly reduced numbers of S436-specific CD8 T cells in the lungs of 12-month-old recipient mice, independent of the source of the transferred cells (Supplemental Figure 2B). Similar results were obtained when cells from 2-month-old and 22-month-old mice were transferred to 2-month-old mice prior to IAV infection (7). Collectively, these results suggest that defects in rDC migration but not in DC- or T cell-intrinsic function are paramount in the diminished T cell response present in infected aged mice.

The nearly complete absence of a SARS-CoV-specific T cell response correlated with decreased survival, so that while 100% of 6-week-old B6 mice infected with 10<sup>4</sup> or 3 × 10<sup>5</sup> PFUs of SARS-CoV survived (Jincun Zhao, unpublished observations), most 12-month-old and all 22-month-old mice infected with 10<sup>4</sup> PFUs succumbed to the infection (Figure 2F). Consistent with the presence of reduced but detectable T cell responses in IAV-infected 22-month-old mice, 60% survived the infection, compared with 90%–100% in 6-week-old to 6-month-old mice (Figure 2G).

*Levels of PGD<sub>2</sub> are elevated in the lungs of aged uninfected and infected mice.* To investigate the basis for diminished rDC migration to DLNs, we initially assessed the role of PGD<sub>2</sub>, a prostaglandin with multiple effects, including the ability to inhibit DC migration under certain conditions (13, 28, 29). First, we measured levels of PGD<sub>2</sub> in the bronchoalveolar lavage fluid (BALF) of uninfected and SARS-CoV- and IAV-infected mice. As shown in Figure 3A, PGD<sub>2</sub> levels increased progressively as mice aged, increasing 3–4 fold in 12-month-old and 22-month-old mice compared with that in 6-week-old mice. Levels at each age were not affected appreciably by OVA-FITC treatment but were modestly increased by infection with IAV (*P* < 0.05, IAV vs. naive at 22 months). Concordant with greater defects in rDC migration in SARS-CoV-infected animals, PGD<sub>2</sub> levels were significantly higher in these mice compared with those in naive or OVA-DQ-treated mice (*P* < 0.05, SARS-CoV vs. naive or OVA-DQ at 12 months and 22 months). In contrast, surface expression of D prostanoid 1 (DP1), the PGD<sub>2</sub> receptor necessary for inhibition of DC migration, was similar on rDCs present in the lungs of SARS-CoV- and IAV-infected mice (Figure 3B).

*Treatment with PGD<sub>2</sub> antagonist enhances rDC migration and T cell proliferation in aged mice.* To determine the functional significance of PGD<sub>2</sub>

**Figure 4**

Treatment with PGD<sub>2</sub> antagonists enhances rDC migration and T cell proliferation in aged mice. (A) Six-week-old or twenty-two-month-old mice were inoculated with 200 μg/75 μl OVA-FITC and PGD<sub>2</sub>, PGE<sub>2</sub>, BW A868C (DP1 receptor antagonist), H89 (PKA antagonist), CAY 10404 (COX-2 antagonist), or CAY 10595 (CRTH2 [DP2] receptor antagonist) i.n., as indicated in the figure. After 18 hours, single-cell suspensions were prepared from lung DLNs and analyzed for the presence of OVA-FITC<sup>+</sup> rDCs. The numbers represent the percentage of OVA-FITC<sup>+</sup> cells within the CD11c<sup>+</sup>MHCII<sup>+</sup> DC population per LN. (B and C) Naive Thy1.1/Thy1.2 OT-I Tg CD8<sup>+</sup> T cells were purified from the spleens of naive mice and labeled with CFSE. (B) A total of 5 × 10<sup>5</sup> or (C) 5 × 10<sup>2</sup> CFSE-labeled T cells were injected i.v. into Thy1.2 recipients. Ten μg OVA-FITC was administered i.n. 24 hours later. After 4 days, DLNs were harvested and analyzed for the presence of CFSE<sup>+</sup>Thy1.1/Thy1.2-positive cells. n = 3–4 mice for each age per experiment. Data are representative of 3 independent experiments. \*P < 0.05.

in regulating rDC migration, we treated young B6 mice i.n. with OVA-FITC and PGD<sub>2</sub>. Migration of rDCs loaded with OVA-FITC decreased 50%–75% after PGD<sub>2</sub> treatment, while exposure to prostaglandin E<sub>2</sub> (PGE<sub>2</sub>), another prostaglandin with a role in inflammation (28, 30), had no significant effect (Figure 4A). We then treated aged mice with drugs that blocked PGD<sub>2</sub> synthesis (CAY 10404, a COX-2 inhibitor), blocked PGD<sub>2</sub> binding to DP1 (BW A868C, specific for PGD<sub>2</sub> and not other PG receptors; ref. 31), or inhibited PGD<sub>2</sub> signaling (H89). All of these treatments, which interfered with PGD<sub>2</sub> function, enhanced rDC migration to the DLNs (Figure 4A). As expected, no enhancement in rDC migration was observed in 6-week-old mice treated with these drugs. DP2, another PGD<sub>2</sub> receptor, is detected primarily on Th2 CD4 T cells (32, 33); treatment with CAY 10595, which blocks DP2 binding, had no effect on rDC migration in aged mice. In subsequent experiments, we used only BW A868C, because it was the most specific of the 3 inhibitors.

To further examine the effects of blocking PGD<sub>2</sub>, we transferred 5 × 10<sup>5</sup> (Figure 4B) or 5 × 10<sup>2</sup> (a more physiological number of cells) (Figure 4C) CFSE-labeled Thy1.1/1.2 OT-I cells (Tg CD8 T cells specific for OVA) to Thy1.2 B6 mice 24 hours prior to treatment with OVA-FITC and BW A868C. Mice were analyzed 4 days later for OT-I proliferation (Figure 4B) or number of cells in the DLN (Figure 4C). OT-I cells proliferated vigorously in 6-week-old mice, and BW A868C did not enhance proliferation. In contrast, proliferation was very modestly decreased in 12-month-old mice and substantially decreased in 24-month-old mice, and, in both cases, BW A868C treatment increased proliferation.

Treatment with PGD<sub>2</sub> antagonist BW A868C enhances rDC migration and T cell responses in SARS-CoV- and IAV-infected mice. Next, we

assessed the role of PGD<sub>2</sub> in the context of infection by treating 12-month-old and 22-month-old SARS-CoV-infected mice and 22-month-old IAV-infected mice with BW A868C. The effect of BW A868C treatment was greatest in SARS-CoV-infected mice. At both 12 months and 22 months, PGD<sub>2</sub> antagonist treatment increased rDC migration to the DLNs (Figure 5A and Supplemental Figure 3A) and the frequency and numbers of total and epitope S436-specific CD8 T cells in lungs (Figure 5B and Supplemental Figure 3B). Blocking PGD<sub>2</sub> function in 12-month-old infected mice enhanced cytolytic activity measured in vivo in infected mice (Figure 5C) and enhanced the kinetics of virus clearance (Figure 5D). These changes resulted in an increase in survival from approximately 10% in 12-month-old infected mice to 70% after BW A868C treatment (Figure 5E). BW A868C also modestly increased survival in 22-month-old infected mice (Supplemental Figure 3C).

Antagonizing PGD<sub>2</sub> function in aged IAV-infected mice also increased rDC migration to the DLN and the numbers of total and PA224-specific CD8 T cells (Figure 6, A and B). These cells were functional, since we also observed an increase in lytic activity using peptide PA224-loaded target cells in an in vivo cytolytic assay after BW A868C treatment (Figure 6C). This enhancement of the PA224-specific response did not result in increased survival, in part, because the NP366-specific CD8 T cell response is most important for protection (1, 34), and, as noted above, there is a hole in the NP366-specific T cell repertoire in aged mice (1). Further, additional defects in the innate immune response (reviewed in ref. 35) are present in 22-month-old mice so that reversal of PGD<sub>2</sub> may be less effective than in younger mice, whether infected with IAV or SARS-CoV (Supplemental Figure 3C).

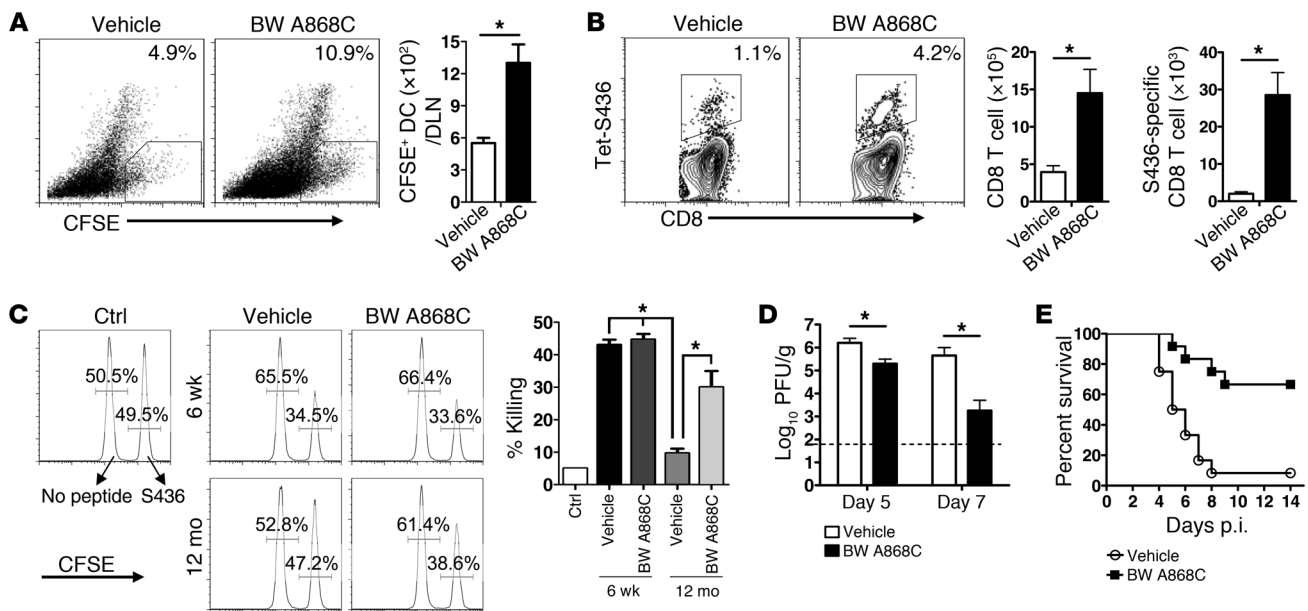


**Figure 5**

Treatment with PGD<sub>2</sub> antagonist BW A868C enhances rDC migration and T cell responses in SARS-CoV-infected mice. (A) Twelve-month-old mice were inoculated i.n. with 50 μl 8 mM CFSE. Six hours after instillation, mice were infected with SARS-CoV together with BW A868C or vehicle. After 18 hours, single-cell suspensions were prepared from lung DLNs (numbers represent the percentage of CFSE<sup>+</sup> cells within the CD11c<sup>+</sup>MHCII<sup>+</sup> DC population). Total CFSE<sup>+</sup> DC numbers per LN are also shown. *n* = 4 mice for each age per experiment. Data are representative of 5 independent experiments. \**P* < 0.05. (B) Lung cells were harvested from 12-month-old B6 mice 6 days after SARS-CoV infection. K<sup>b</sup>/S436 tetramer staining and total numbers of CD8 T cells and of K<sup>b</sup>/S436 tetramer<sup>+</sup> CD8 T cells are shown. Numbers represent the percentages of tetramer<sup>+</sup> CD8 T cells. *n* = 4–6 mice/group/experiment. Data are representative of 7 independent experiments. \**P* < 0.05. (C) In vivo cytotoxicity assays were performed on day 6 p.i., and the percentage of killing was calculated, as described in Methods (numbers represent the percentage of cells labeled with different concentrations of CFSE). *n* = 4–6 mice/group/experiment. Data are representative of 2 independent experiments. \**P* < 0.05. Twelve-month-old mice were i.n. infected with 1 × 10<sup>4</sup> PFUs SARS-CoV virus with or without BW A868C. (D) Viral titers are expressed as PFU/g tissue. *n* = 4 mice/group/time point. Data are representative of 2 independent experiments. \**P* < 0.05. (E) Mortality was monitored daily. *n* = 12 mice in vehicle group; *n* = 12 mice in BW A868C group. *P* = 0.0007, determined by a Kaplan-Meier survival test.

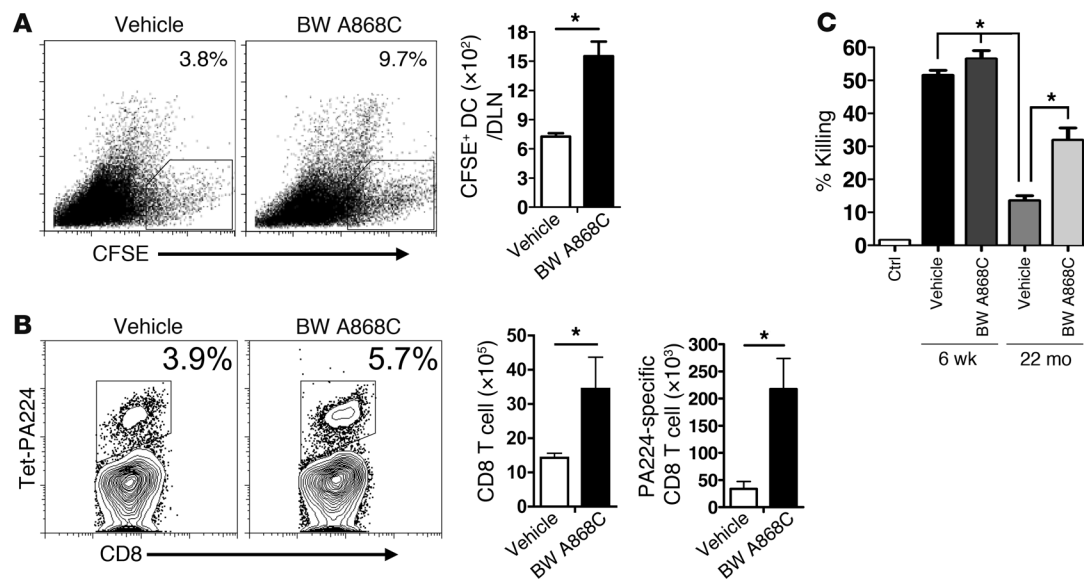
Antibody responses are a critical component of the immune response to IAV and other pathogens. We next determined whether there were age-dependent deficiencies in antibody responses to SARS-CoV and IAV and whether any defects were reversed by BW A868C treatment. Anti-SARS-CoV antibody titers were measured at 6 days p.i., before significant mortality in the vehicle-treated group occurred. Titers were nearly the same in 6-week-old and 12-month-old infected mice and were not increased by PGD<sub>2</sub> antagonism (Supplemental Methods and Supplemental Figure 4A). In contrast, IAV hemagglutination inhibition titers were decreased in 22-month-old compared with 6-week-old infected mice, but BW A868C treatment did not enhance titers in either age group (Supplemental Methods and Supplemental Figure 4B).

*Changes in CCR7 expression correlate with enhanced rDC migration.* Blocking PGD<sub>2</sub> may enhance the proinflammatory milieu in the lungs, contributing to enhanced rDC migration. However, PGD<sub>2</sub> antagonist treatment did not change lung mRNA levels of several molecules associated with inflammation (*Il1b*, *Tnf*, *Il6*, *Thr3*, *Thr7*, *Csf2*, and *Il12*) (Figure 7, A and B). CCR7 is a chemokine receptor implicated in DC migration to the DLN (11, 36). Strikingly, PGD<sub>2</sub> antagonism resulted in increased numbers of rDCs expressing CCR7 in the lung at very early times (~10 hour) p.i. (Figure 7, C and D), when rDC migration to DLN is just beginning (Figure 1). In contrast, similar numbers of CCR7<sup>+</sup> rDCs were detected in the

lungs of treated and control mice by 18 hours p.i., reflecting the peak of rDC migration to the DLN. A previous study showed that PGD<sub>2</sub> diminished DC expression of CCR7 in vitro (37). In agreement with this study, we observed diminished CCR7 expression on rDCs in the DLNs of SARS-CoV-infected 12-month-old mice and IAV-infected 22-month-old mice when compared with that of their infected 6-week-old counterparts (Figure 7, E and F). BW A868C treatment significantly increased CCR7 expression on rDCs isolated from DLNs of aged mice, consistent with a role in enhanced migration from the lungs.

**Discussion**

Specific intrinsic defects in T cell function in pulmonary viral infections in older individuals have been well described (1, 38–40). Our results indicate that another major contributory factor to suboptimal T cell function in older populations is the impaired capacity of rDCs to migrate to DLNs and also demonstrate that the degree of impairment is pathogen-specific. Defects in rDC migration occur progressively as mice age. For most infections, such as those caused by IAV or RSV, they do not significantly impact antiviral T cell responses and virus clearance until mice are very old (>20 months). With some infections, such as those caused by SARS-CoV, rDC migration defects occur at earlier times after infection, causing more severe disease at a younger age. These results are

**Figure 6**

Treatment with PGD<sub>2</sub> antagonist BW A868C enhances rDC migration and T cell responses in IAV-infected mice. **(A)** Twenty-two-month-old mice were inoculated i.n. with 50  $\mu$ l 8 mM CFSE. Six hours after instillation, mice were infected with IAV together with BW A868C or vehicle. After 18 hours, single-cell suspensions were prepared from lung DLNs. The values represent the percentages of CFSE<sup>+</sup> cells within the CD11c<sup>+</sup>MHCII<sup>+</sup> DC population. Total CFSE<sup>+</sup> DC numbers per LN are also shown.  $n = 4$  mice for each age per experiment. Data are representative of 4 independent experiments. \* $P < 0.05$ . **(B)** Lung cells were harvested from 22-month-old B6 mice 8 days after IAV infection. D<sup>b</sup>/PA224 tetramer staining and total numbers of CD8 T cells and of D<sup>b</sup>/PA224 tetramer<sup>+</sup> CD8 T cells are shown. Numbers represent the percentages of tetramer<sup>+</sup> CD8 T cells.  $n = 4$ –6 mice/group/experiment. Data are representative of 5 independent experiments. \* $P < 0.05$ . **(C)** In vivo cytotoxicity assays were performed on day 7 p.i., and the percentage of killing was calculated, as described in Methods.  $n = 4$ –6 mice/group/experiment. Data are representative of 2 independent experiments. \* $P < 0.05$ .

consistent with observations made during the 2002–2003 SARS epidemic. While no mortality was observed in individuals under 24 years of age, 6%, 15%, and 52% of young (25–44 years), middle-aged (45–64 years), and aged (>65 years) patients, respectively, succumbed to the infection (6).

Our results provide an explanation for these rDC migration defects. We show that levels of PGD<sub>2</sub> in the lung increased as mice aged and further increased after viral infection (Figure 3A). In addition, SARS-CoV increased PGD<sub>2</sub> to a greater extent than IAV, especially in 12-month-old mice ( $P < 0.05$ ). Viruses interact with multiple host cell proteins and pathways as part of their replication strategies (41–44). It is likely that some host cell proteins will be important for replication of all viruses, whereas others will be used in a virus-specific manner. Enhancement of PGD<sub>2</sub> levels would be advantageous for virus replication. While IAV and SARS-CoV both increase PGD<sub>2</sub> synthesis or accumulation, our results are consistent with the notion that a SARS-CoV protein efficiently interacts with the PGD<sub>2</sub> pathway, although determining the molecular basis of this effect will require additional work.

PGD<sub>2</sub>, expressed by a variety of cell types, including mast cells, macrophages, DCs, epithelial cells, and Th2 CD4 T cells, has both proinflammatory and antiinflammatory effects (12, 13, 28, 33, 45). The role of PGD<sub>2</sub> is well characterized in asthma and other allergic diseases in which PGD<sub>2</sub> is produced primarily by mast cells and acts as a proinflammatory mediator enhancing the function of Th2 CD4 T cells through binding to CRTH2 (chemoattractant receptor-homologous molecules expressed on Th2 cells) receptors (13, 33). While mast cells produce the largest amounts of PGD<sub>2</sub> when

measured on a per cell basis, it is likely that DCs, macrophages, and respiratory tract epithelial cells are the major sources for PGD<sub>2</sub> in the lungs of virus-infected mice. PGD<sub>2</sub> also has antiinflammatory effects, with inhibitory effects on Th1 CD4 T cell function, monocyte/macrophage and dendritic migration and differentiation, and IL-12 production (13). These effects are mediated by binding to DP1 and intracellular PPAR $\gamma$  receptors (28, 29). We showed that blockade of the DP1 receptor suppressed the effects of PGD<sub>2</sub>, suggesting that signaling through this receptor is most important in regulating rDC migration in the virus-infected lung (Figures 5 and 6). Signaling through this receptor is also involved in the uninfected lung, since BW A868C enhanced migration of OVA-FITC-labeled rDCs to the DLNs (Figure 4A), while exogenously delivered PGD<sub>2</sub> diminished rDC migration to the DLNs (23).

Our results also suggest that PGD<sub>2</sub> functions, in part, by inhibiting CCR7 upregulation (Figure 7, C–F), thereby hindering rDC migration to DLNs. While CCR7 is critical for DC migration to DLNs, its upregulation by itself is not sufficient for maximal DC chemotaxis (11, 36, 46), suggesting that additional activation signals are required. Of note, CCR7 ligation with its ligands (CCL19 and CCL21), in addition to increasing rDC migration, increases DC survival and enhances other DC functions, such as migratory speed, levels of MHC and costimulatory molecules, and rate of endocytosis, all of which are predicted to contribute to an enhanced T cell response in the aged lung (reviewed in ref. 36). The ability of PGD<sub>2</sub> to dampen DC migration from the skin is used by the helminth parasite, *Schistoma mansoni*, to evade the host immune response and thereby facilitate parasite growth (47, 48).

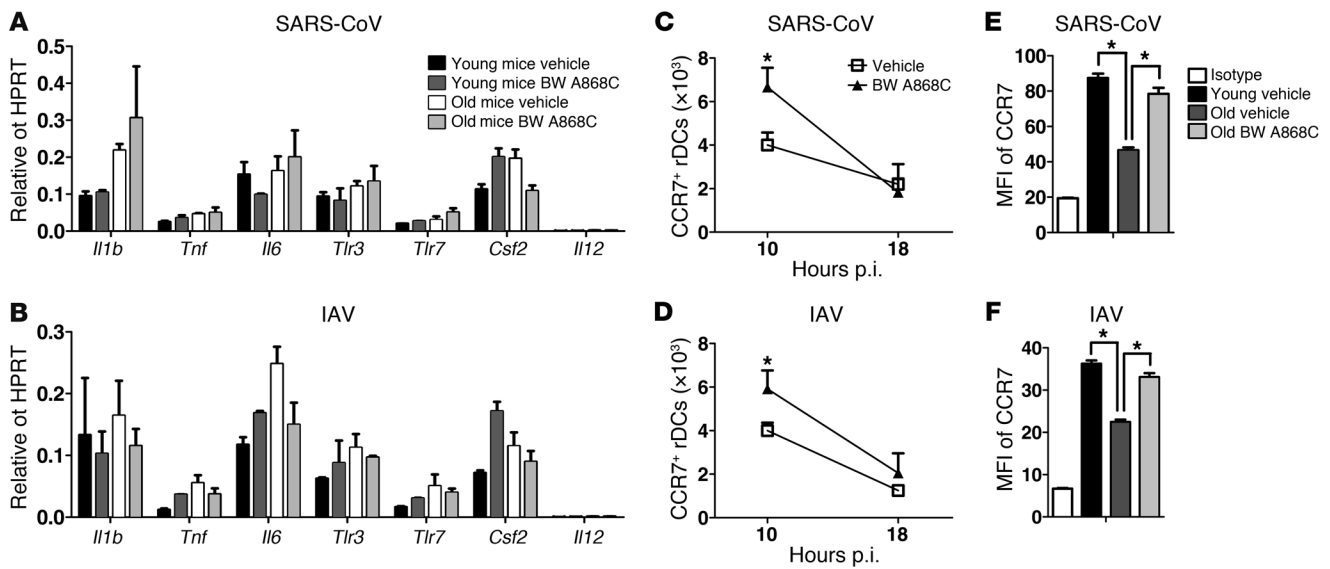


**Figure 7** Cytokine and chemokine RNA and CCR7 levels in young and aged mice after SARS-CoV or IAV infection and BW A868C treatment. (A and B) Cytokine and chemokine RNA levels in infected lungs. RNA was extracted from (A) SARS-CoV- or (B) IAV-infected lungs 18 hours p.i. and processed, as described in Methods. *n* = 4 mice/group/experiment. Data are representative of 2 independent experiments. (C and D) Numbers of CD11c<sup>+</sup>MHCII<sup>+</sup> SiglecF<sup>-</sup> rDCs expressing CCR7 in (C) SARS-CoV- and (D) IAV-infected lungs at 10 and 18 hours p.i. (E and F) CCR7 expression on migratory rDCs in DLNs. Young and aged mice were inoculated i.n. with 50  $\mu$ l 8 mM CFSE. Six hours after instillation, mice were infected with (E) SARS-CoV (6 weeks old and 12 months old) or (F) IAV (6 weeks old and 22 months old), together with BW A868C. After 18 hours single-cell suspensions were prepared from lung DLNs. CCR7 expression levels on the CFSE<sup>+</sup>CD11c<sup>+</sup>MHCII<sup>+</sup> DC population are shown. *n* = 4–6 mice/group. Data are representative of 5–6 independent experiments. \**P* < 0.05.

By expressing PGD<sub>2</sub>, the parasite retains Langerhans cells at the site of infection, hindering the development of an effective T cell response. PGD<sub>2</sub> also has other functions, including augmentation of neutrophil migration into sites of inflammation (49). Consistent with this, there are increased numbers of neutrophils in the lungs of aged mice infected with IAV (50) or SARS-CoV (Jincun Zhao, unpublished observations).

Collectively, these results suggest that inhibition of PGD<sub>2</sub> may enhance T cell responses and clinical outcomes in older patients with severe respiratory viral infections if delivered at very early times in the disease course. Further, our results raise the intriguing possibility that treatment with PGD<sub>2</sub> antagonists will enhance the immune response to vaccines. In particular, the cold-adapted live-attenuated influenza A vaccine (LAIV), which is administered i.n., is not approved for individuals older than 49 years of age and is less immunogenic than inactivated IAV (51). If this diminished immunogenicity reflects deficiencies in DC migration, PGD<sub>2</sub> antagonist treatment at the time of live-attenuated influenza A vaccination might reverse such defects and increase vaccine efficacy, which would be especially relevant in aged populations. PGD<sub>2</sub> antagonists, such as laropiprant (52–54), have been used in patients, suggesting the feasibility of this approach.

**Methods**

**Mice and viruses.** Pathogen-free B6 mice, with ages ranging from 6 weeks to 24 months, were purchased from the National Cancer Institute and National Institute on Aging. Thy1.1 B6 congenic mice and OT-I Tg mice on a B6 background were provided by J. Harty (Department of Microbiology, University of Iowa). Mice were maintained in the animal care facility at the University of Iowa. Mouse-adapted SARS-CoV (MA15) was a gift from

Kanta Subbarao (NIH, Bethesda, Maryland, USA) (55). Mouse-adapted IAV A/PR/8/34 was grown in the allantoic fluid of 10-day-old embryonated chicken eggs for 2 days at 37°C, as previously described (56). RSV (A2 strain) was a gift from S. Varga (Department of Microbiology, University of Iowa). MHV-1 was purchased from ATCC and propagated in 17Cl-1 cells.

**Peptides, tetramer, and chemicals.** SARS-CoV-specific peptide, S436 (HNYKYRYL), and IAV-specific peptides, PA224 (SSLENFRAYV) and NP366 (ASNENMETM), were synthesized by BioSynthesis Inc. H2K<sup>b</sup>/S436, H2D<sup>b</sup>/PA224, and H2D<sup>b</sup>/NP366 tetramers were obtained from the National Institute of Allergy and Infectious Disease MHC Tetramer Core Facility. PGD<sub>2</sub>, PGE<sub>2</sub>, BW A868C (DP1 receptor antagonist), H89 (PKA antagonist), Cay 10404 (COX-2 antagonist), and Cay 10595 (DP2 receptor antagonist) were purchased from Cayman Chemical and reconstituted as suggested by the manufacturer.

**Virus infection and titration.** B6 mice were lightly anesthetized with isoflurane and infected i.n. with 1  $\times$  10<sup>4</sup> PFUs of SARS-CoV, 1,066 tissue culture infectious units of IAV, 3  $\times$  10<sup>6</sup> PFUs of RSV, or 3  $\times$  10<sup>5</sup> PFUs of MHV-1 in a total volume of 50  $\mu$ l DMEM medium. For some experiments, mice were inoculated with virus together with 10 nM PGD<sub>2</sub> or its antagonists. Mice were monitored daily for mortality. All work with SARS-CoV was conducted in the University of Iowa Biosafety Level 3 Laboratory. To obtain SARS-CoV titers, lungs were removed into PBS and titered on Vero E6 cells, as previously described (57). Viral titers are expressed as PFU per g tissue.

**In situ CFSE, OVA-FITC, and OVA-DQ staining.** CFSE, OVA-FITC, and OVA-DQ were purchased from Molecular Probes. CFSE was dissolved at 25 mM in DMSO and stored at -80°C until use. CFSE was diluted in DMEM to a concentration of 8 mM and then administered i.n. (50  $\mu$ l/mouse) following anesthesia with isoflurane 6 hours before infection (18). OVA-FITC and OVA-DQ were dissolved in PBS and administered i.n. (200  $\mu$ g/75  $\mu$ l/mouse) with or without PGD<sub>2</sub> or its antagonists follow-



ing isoflurane anesthesia. Of note, OVA-DQ acquires fluorescence after dequenching through proteolytic enzyme cleavage, permitting analyses of both antigen uptake and processing.

**Preparation of cells from lungs and DLNs.** Mice were sacrificed at the indicated time points. The lung vascular bed was flushed via the right ventricle with 5 ml PBS, and lungs and DLNs were then removed. Lungs were cut into small pieces and digested in HBSS buffer containing 2% FCS, 25 mM HEPES, 1 mg/ml Collagenase D (Roche), and 0.1 mg/ml DNase (Roche) for 30 minutes at room temperature. LNs were minced and pressed through a wire screen. Particulate matter was removed with a 70- $\mu$ m nylon filter to obtain single-cell suspensions. Cells were enumerated by 0.2% trypan blue exclusion.

**Antibodies and flow cytometry.** The following monoclonal antibodies were used for these studies: rat anti-mouse CD4 (RM4-5), rat anti-mouse CD8 $\alpha$  (53-6.7), rat anti-mouse Thy1.1 (OX-7), rat anti-mouse CD11b (M1/70), hamster anti-mouse CD11c (HL3), rat anti-mouse CD16/32 (2.4G2), rat anti-mouse Siglec F (E50-2440), and rat anti-mouse CD40 (1C10), all from BD Biosciences; rat anti-mouse IFN- $\gamma$  (XMG1.2), rat anti-mouse CCR7 (4B12), and hamster anti-CD103 (2E7), all from eBioscience; rat anti-mouse Thy1.2 (30-H12), rat anti-mouse CD86 (GL-1), and rat anti-mouse I-A/I-E (M5/114.15.2), all from Biolegend; and rabbit anti-mouse DP1 receptor polyclonal antibody and goat anti-rabbit IgG Surelight APC, both from Cayman Chemical.

For surface staining,  $10^6$  cells were blocked with 1  $\mu$ g anti-CD16/32 antibody and 1% rat serum and stained with the indicated antibodies at 4°C, except for those stained with CCR7, which were stained at 37°C. Cells were then fixed using Cytofix Solution (BD Biosciences). For tetramer staining, cells were stained for 30 minutes at 4°C. Cells were then incubated with surface staining antibodies. For intracellular cytokine staining,  $1 \times 10^6$  cells per well were cultured in 96-well dishes at 37°C for 5 to 6 hours in the presence of Brefeldin A (BD Biosciences). Cells were then labeled with surface antibodies, fixed/permeabilized with Cytofix/Cytoperm Solution (BD Biosciences), and labeled with anti-IFN- $\gamma$  antibody. To detect DP1 receptor, cells were fixed with Cytofix/Cytoperm and stained with 2  $\mu$ g/ml polyclonal rabbit anti-DP1 receptor antibody for 1 hour at room temperature and then incubated with goat anti-rabbit IgG Surelight APC for 1 hour. All flow cytometry data were acquired on a BD FACSCalibur or an LSR II (BD Biosciences) and were analyzed using FlowJo software (Tree Star Inc.).

**Adoptive transfer of splenocytes.** Naive Thy1.1/Thy1.2 OT-I Tg CD8 $^+$  T cells were harvested from the spleens of uninfected mice and labeled with 2.5  $\mu$ M CFSE. A total of  $5 \times 10^5$  or  $5 \times 10^2$  CFSE-labeled T cells were injected i.v. into the tail veins of Thy1.2 recipients. Ten  $\mu$ g of OVA-FITC were administered i.n. 24 hours later. After 4 days, DLNs were harvested and analyzed for CFSE- and Thy1.1/Thy1.2-positive cells.

**Enzyme immunoassay for PGD<sub>2</sub>.** Lungs were inflated with cold PBS via cannulation of the trachea and were lavaged 3 times. BALFs were pooled and aliquoted and stored at -80°C. Enzyme immunoassay was used to quantify PGD<sub>2</sub> levels in the BALF, following the manufacturer's instructions (Cayman Chemical).

**In vivo cytotoxicity assay.** In vivo cytotoxicity assays were performed on day 6–7 after infection, as previously described (58). Briefly, splenocytes from naive mice were costained with PKH26 (Sigma-Aldrich) and either 1  $\mu$ M or 100 nM CFSE (Molecular Probes). Labeled cells were then pulsed with the indicated peptides (10  $\mu$ M) at 37°C for 1 hour, and  $5 \times 10^5$  cells from each group were mixed together ( $1 \times 10^6$  cells in total). Cells were transferred i.n. into mice, and total lung cells were isolated at 12 hours after transfer. Target cells were distinguished from host cells on the basis of PKH26 staining and from each other on the basis of CFSE staining. After gating on PKH26 $^+$  cells, the percentage of killing was calculated, as previously described (58).

**Cytokine and chemokine RNA levels in infected lungs using qRT-PCR.** RNA was extracted from infected lungs 18 hours p.i. using TRIzol (Invitrogen), and 2  $\mu$ g RNA was used as a template for cDNA synthesis (Invitrogen). Two microliters of cDNA were added to a 23  $\mu$ l PCR cocktail containing 2 $\times$ SYBR Green Master Mix (ABI) and 0.2  $\mu$ M of each sense and antisense primer (IDT DNA). Amplification was performed in an ABI Prism 7700 thermocycler. Specific primer sets used for assaying cytokine and house-keeping gene expression were previously described (59, 60).

**Statistics.** A Student's *t* test was used to analyze differences in mean values between groups. All results are expressed as mean  $\pm$  SEM. *P* values of less than 0.05 were considered statistically significant. Differences in mortality were analyzed using Kaplan-Meier log-rank survival tests.

**Study approval.** All animal studies were approved by the University of Iowa Animal Care and Use Committee and meet stipulations of the Guide for the Care and Use of Laboratory Animals (NIH).

## Acknowledgments

We thank John Harty for critical review of the manuscript. This research was supported in part by grants from the NIH (PO1 AI060699, R56 AI79424, and RO1 AI091322 to S. Perlman and RO1 AI071085 to K. Legge).

Received for publication June 30, 2011, and accepted in revised form October 5, 2011.

Address correspondence to: Stanley Perlman, Department of Microbiology, University of Iowa, 51 Newton Road, BSB 3-712, Iowa City, Iowa 52242, USA. Phone: 319.335.8549; Fax: 319.335.9006; E-mail: Stanley-perlman@uiowa.edu.

1. Yager EJ, Ahmed M, Lanzer K, Randall TD, Woodland DL, Blackman MA. Age-associated decline in T cell repertoire diversity leads to holes in the repertoire and impaired immunity to influenza virus. *J Exp Med*. 2008;205(3):711–723.
2. Brien JD, Uhrlaub JL, Hirsch A, Wiley CA, Nikolich-Zugich J. Key role of T cell defects in age-related vulnerability to West Nile virus. *J Exp Med*. 2009;206(12):2735–2745.
3. Rockx B, et al. Early upregulation of acute respiratory distress syndrome-associated cytokines promotes lethal disease in an aged-mouse model of severe acute respiratory syndrome coronavirus infection. *J Virol*. 2009;83(14):7062–7074.
4. Nagata N, et al. Mouse-passaged severe acute respiratory syndrome-associated coronavirus leads to lethal pulmonary edema and diffuse alveolar damage in adult but not young mice. *Am J Pathol*. 2008;172(6):1625–1637.
5. Katz JM, Plowden J, Renshaw-Hoelscher M, Lu X, Tumpey TM, Sambhara S. Immunity to influenza: the challenges of protecting an aging population. *Immunol Res*. 2004;29(1–3):113–124.
6. Peiris JS, Guan Y, Yuen KY. Severe acute respiratory syndrome. *Nat Med*. 2004;10(12 suppl):S88–S97.
7. Linton PJ, Li SP, Zhang Y, Bautista B, Huynh Q, Trinh T. Intrinsic versus environmental influences on T-cell responses in aging. *Immunol Rev*. 2005; 205:207–219.
8. Plackett TP, Boehmer ED, Faunce DE, Kovacs EJ. Aging and innate immune cells. *J Leukoc Biol*. 2004;76(2):291–299.
9. Shurin MR, Shurin GV, Chatta GS. Aging and the dendritic cell system: implications for cancer. *Crit Rev Oncol Hematol*. 2007;64(2):90–105.
10. Agrawal A, Agrawal S, Tay J, Gupta S. Biology of dendritic cells in aging. *J Clin Immunol*. 2008;28(1):14–20.
11. Randolph GJ, Ochoaño J, Partida-Sanchez S. Migration of dendritic cell subsets and their precursors. *Annu Rev Immunol*. 2008;26:293–316.
12. Narumiya S. Prostanoids and inflammation: a new concept arising from receptor knockout mice. *J Mol Med*. 2009;87(10):1015–1022.
13. Kim N, Luster AD. Regulation of immune cells by eicosanoid receptors. *Scientific World Journal*. 2007; 7:1307–1328.
14. Hopken UE, Lipp M. All roads lead to Rome: triggering dendritic cell migration. *Immunity*. 2004; 20(3):244–246.
15. Jakubzick C, Tacke F, Llodra J, van Rooijen N, Randolph GJ. Modulation of dendritic cell trafficking to and from the airways. *J Immunol*. 2006; 176(6):3578–3584.
16. Thompson WW, et al. Mortality associated with influenza and respiratory syncytial virus in the United States. *JAMA*. 2003;289(2):179–186.
17. De Albuquerque N, et al. Murine hepatitis virus strain 1 produces a clinically relevant model of severe acute respiratory syndrome in A/J mice. *J Virol*. 2006; 80(21):10382–10394.
18. Legge KL, Braciale TJ. Accelerated migration of respiratory dendritic cells to the regional lymph nodes is limited to the early phase of pulmonary



- infection. *Immunity*. 2003;18(2):265–277.
19. Silvana Dos Santos S, Ferreira KS, Almeida SR. Paracoccidioides brasiliensis-induced migration of dendritic cells and subsequent T-cell activation in the lung-draining lymph nodes. *PLoS One*. 2011;6(5):e19690.
20. McWilliam AS, Nelson D, Thomas JA, Holt PG. Rapid dendritic cell recruitment is a hallmark of the acute inflammatory response at mucosal surfaces. *J Exp Med*. 1994;179(4):1331–1336.
21. Vermaelen KY, Carro-Muino I, Lambrecht BN, Pauwels RA. Specific migratory dendritic cells rapidly transport antigen from the airways to the thoracic lymph nodes. *J Exp Med*. 2001;193(1):51–60.
22. Ballesteros-Tato A, Leon B, Lund FE, Randall TD. Temporal changes in dendritic cell subsets, cross-priming and costimulation via CD70 control CD8(+) T cell responses to influenza. *Nat Immunol*. 2010;11(3):216–224.
23. Hammad H, de Heer HJ, Soullie T, Hoogsteden HC, Trottein F, Lambrecht BN. Prostaglandin D2 inhibits airway dendritic cell migration and function in steady state conditions by selective activation of the D prostanoid receptor 1. *J Immunol*. 2003;171(8):3936–3940.
24. Sung SS, Fu SM, Rose CE Jr, Gaskin F, Ju ST, Beatty SR. A major lung CD103 (alphaE)-beta7 integrin-positive epithelial dendritic cell population expressing Langerin and tight junction proteins. *J Immunol*. 2006;176(4):2161–2172.
25. Beatty SR, Rose CE Jr, Sung SS. Diverse and potent chemokine production by lung CD11bhigh dendritic cells in homeostasis and in allergic lung inflammation. *J Immunol*. 2007;178(3):1882–1895.
26. del Rio ML, Rodriguez-Barbosa JJ, Kremmer E, Forster R. CD103- and CD103+ bronchial lymph node dendritic cells are specialized in presenting and cross-presenting innocuous antigen to CD4+ and CD8+ T cells. *J Immunol*. 2007;178(11):6861–6866.
27. Kim TS, Braciale TJ. Respiratory dendritic cell subsets differ in their capacity to support the induction of virus-specific cytotoxic CD8+ T cell responses. *PLoS One*. 2009;4(1):e4204.
28. Scher JU, Pillinger MH. The anti-inflammatory effects of prostaglandins. *J Invest Med*. 2009;57(6):703–708.
29. Sandig H, Pease JE, Sabroe I. Contrary prostaglandins: the opposing roles of PGD2 and its metabolites in leukocyte function. *J Leukoc Biol*. 2007;81(2):372–382.
30. Vancheri C, Mastruzzo C, Sortino MA, Crimi N. The lung as a privileged site for the beneficial actions of PGE2. *Trends Immunol*. 2004;25(1):40–46.
31. Giles H, Leff P, Bololo ML, Kelly MG, Robertson AD. The classification of prostaglandin DP-receptors in platelets and vasculature using BW A868C, a novel, selective and potent competitive antagonist. *Br J Pharmacol*. 1989;96(2):291–300.
32. Nagata K, et al. CRTH2, an orphan receptor of T-helper-2-cells, is expressed on basophils and eosinophils and responds to mast cell-derived factor(s). *FEBS Lett*. 1999;459(2):195–199.
33. Pettipher R, Hansel TT, Armer R. Antagonism of the prostaglandin D2 receptors DP1 and CRTH2 as an approach to treat allergic diseases. *Nat Rev Drug Discov*. 2007;6(4):313–325.
34. Crowe SR, et al. Differential antigen presentation regulates the changing patterns of CD8+ T cell immunodominance in primary and secondary influenza virus infections. *J Exp Med*. 2003;198(3):399–410.
35. Kovacs EJ, Palmer JL, Fortin CF, Fulop T Jr, Goldstein DR, Linton PJ. Aging and innate immunity in the mouse: impact of intrinsic and extrinsic factors. *Trends Immunol*. 2009;30(7):319–324.
36. Sanchez-Sanchez N, Riol-Blanco L, Rodriguez-Fernandez JL. The multiple personalities of the chemokine receptor CCR7 in dendritic cells. *J Immunol*. 2006;176(9):5153–5159.
37. Gosset P, Pichavant M, Faveuw C, Bureau F, Tonnel AB, Trottein F. Prostaglandin D2 affects the differentiation and functions of human dendritic cells: impact on the T cell response. *Eur J Immunol*. 2005;35(5):1491–1500.
38. Meyer KC. The role of immunity and inflammation in lung senescence and susceptibility to infection in the elderly. *Semin Respir Crit Care Med*. 2010;31(5):561–574.
39. Ely KH, Roberts AD, Kohlmeier JE, Blackman MA, Woodland DL. Aging and CD8+ T cell immunity to respiratory virus infections. *Exp Gerontol*. 2007;42(5):427–431.
40. Murasko DM, Jiang J. Response of aged mice to primary virus infections. *Immunol Rev*. 2005;205:285–296.
41. Karlas A, et al. Genome-wide RNAi screen identifies human host factors crucial for influenza virus replication. *Nature*. 2010;463(7282):818–822.
42. Konig R, et al. Human host factors required for influenza virus replication. *Nature*. 2010;463(7282):813–817.
43. Shapira SD, et al. A physical and regulatory map of host-influenza interactions reveals pathways in H1N1 infection. *Cell*. 2009;139(7):1255–1267.
44. Krishnan MN, et al. RNA interference screen for human genes associated with West Nile virus infection. *Nature*. 2008;455(7210):242–245.
45. Copland IB, Reynaud D, Pace-Asciak C, Post M. Mechanotransduction of stretch-induced prostanoid release by fetal lung epithelial cells. *Am J Physiol Lung Cell Mol Physiol*. 2006;291(3):L487–L495.
46. Bouchon A, Hernandez-Munain C, Cella M, Colonna M. A DAP12-mediated pathway regulates expression of CC chemokine receptor 7 and maturation of human dendritic cells. *J Exp Med*. 2001;194(8):1111–1122.
47. Angeli V, et al. Role of the parasite-derived prostaglandin D2 in the inhibition of epidermal Langerhans cell migration during schistosomiasis infection. *J Exp Med*. 2001;193(10):1135–1147.
48. Herve M, et al. Pivotal roles of the parasite PGD2 synthase and of the host D prostanoid receptor 1 in schistosome immune evasion. *Eur J Immunol*. 2003;33(10):2764–2772.
49. Tull SP, et al. Omega-3 Fatty acids and inflammation: novel interactions reveal a new step in neutrophil recruitment. *PLoS Biol*. 2009;7(8):e1000177.
50. Toapanta FR, Ross TM. Impaired immune responses in the lungs of aged mice following influenza infection. *Respir Res*. 2009;10:112.
51. Monto AS, et al. Comparative efficacy of inactivated and live attenuated influenza vaccines. *N Engl J Med*. 2009;361(13):1260–1267.
52. Sturino CF, et al. Discovery of a potent and selective prostaglandin D2 receptor antagonist, [(3R)-4-(4-chloro-benzyl)-7-fluoro-5-(methylsulfonyl)-1,2,3,4-tetrahydrocyclopent a[b]indol-3-yl]-acetic acid (MK-0524). *J Med Chem*. 2007;50(4):794–806.
53. Paolini JF, et al. Effects of laropiprant on nicotinic acid-induced flushing in patients with dyslipidemia. *Am J Cardiol*. 2008;101(5):625–630.
54. Sanyal S, Kuvin JT, Karas RH. Niacin and laropiprant. *Drugs Today (Barc)*. 2010;46(6):371–378.
55. Roberts A, et al. A mouse-adapted SARS-coronavirus causes disease and mortality in BALB/c mice. *PLoS Pathog*. 2007;3(1):e5.
56. Legge KL, Braciale TJ. Lymph node dendritic cells control CD8+ T cell responses through regulated FasL expression. *Immunity*. 2005;23(6):649–659.
57. Zhao J, Van Rooijen N, Perlman S. Evasion by stealth: inefficient immune activation underlies poor T cell response and severe disease in SARS-CoV-infected mice. *PLoS Pathog*. 2009;5(10):e1000636.
58. Barber DL, Wherry EJ, Ahmed R. Cutting edge: rapid in vivo killing by memory CD8 T cells. *J Immunol*. 2003;171(1):27–31.
59. Trandem K, Zhao J, Fleming E, Perlman S. Highly activated cytotoxic CD8 T cells express protective IL-10 at the peak of coronavirus-induced encephalitis. *J Immunol*. 2011;186(6):3642–3652.
60. Zhou H, Zhao J, Perlman S. Autocrine interferon priming in macrophages but not dendritic cells results in enhanced cytokine and chemokine production after coronavirus infection. *MBio*. 2010;1(4):e00219-10.